ARTICLE NO. 80-4120

Frequency-Shaped Cost Functionals: Extension of Linear-Quadratic-Gaussian Design Methods

Narendra K. Gupta*
Integrated Systems, Inc., Palo Alto, Calif.

The linear-quadratic-Gaussian method for feedback control design is extended to include frequency-shaped weighting matrices in the quadratic cost functional. This extension provides a means to meet classical design requirements with automated computational procedures of modern control theory. A design algorithm to optimize frequency-shaped cost functionals requires definition of new states and the solution of a modified linear-quadratic-Gaussian problem. Four examples are presented to demonstrate frequency shaping methodology: 1) aircraft in lateral wind, 2) an industrial crane, 3) vibration control in helicopters, and 4) a system with truncated modes.

I. Introduction

THE *modern control theory* method of linear-quadratic-Gaussian (LQG) design is based on linear model, Gaussian noise, and quadratic performance index. The state variable model is

$$\dot{x}=Fx+Gu+w \qquad x(0)=x_0 \qquad (0\le t\le t_f) \tag{1}$$

where x is an $n\times 1$ state vector, u is a $q\times 1$ control vector, and w is $n\times 1$ Gaussian noise with mean zero and intensity Q. The control u is selected to minimize

$$J=\int_0^{t_f}(x^TAx+u^TBu)\,dt+x^T(t_f)S_fx(t_f) \tag{2}$$

A is a positive semidefinite matrix and B is a positive definite matrix. The optimal control law is linear.[1]

$$u^*(t)=C(t)x(t) \tag{3}$$

$C(t)$ is explicitly obtained by solving the following Riccati equation:

$$\dot{S}=F^TS-SF-A+SGB^{-1}G^TS \qquad S(t_f)=S_f \tag{4}$$

$$C(t)=-B^{-1}G^TS \tag{5}$$

This equation must be solved backward in time. The control law is dependent on system definition matrices F and G and performance index weighting matrices A, B, and S_f. The control gain $C(t)$ is a function of time.

As $T\to\infty$, the solution to Eq. (4) reaches a steady state. The steady-state solution satisfies the algebraic Riccati equation (ARE):

$$-F^TS-SF-A+SGB^{-1}G^TS=0 \tag{6}$$

The feedback control signal requires all system states which, in general, are not measured. The states may be estimated by using an observer with measurements $y(t)$ which are contaminated with noise v

$$y=Hx+v \tag{7}$$

$$\dot{\hat{x}}=F\hat{x}+Gu+K(y-H\hat{x}) \tag{8}$$

In Eq. (8), $\hat{x}$ is an estimate of the state vector and K is selected to minimize estimation error based on the process and measurement noise. The control law is modified to use the estimated state vector instead of the real state.

$$u=C\hat{x} \tag{9}$$

It is clear from the above that the modern control theory is based on optimization methods with a specified model form. The feedback system behaves well under the following conditions:

1) The model is valid for all values of inputs and states. In addition, the dynamics are well-described at all input and state frequencies.

2) The filter design also assumes that the dynamics is known equally accurately at all frequencies. (The filter uses values of F, G, and H matrices explicitly in addition to the gain K which also depends on the state definition matrices.) This may make the combination of the filter and the control law extremely sensitive to errors (see also Ref. 2).

3) The optimality of the filter is strongly dependent on the accuracy of noise statistics.

Classical control design methods are based on frequency domain descriptions of systems and often account for model uncertainty at high frequencies by the use of gain and phase margins that are larger than those needed if the model were certain. The system dynamics may be described in terms of the output-input transfer function (s is the Laplace variable)

$$y(s)=T(s)u(s) \tag{10}$$

Bode plots, Nyquist diagrams, or other frequency domain methods are used to develop a feedback compensator. In general, the control law is of the form

$$u(s)=C_c(s)y(s) \tag{11}$$

For single-input, single-output systems, the compensator $C_c(s)$ is obtained through the use of root-locus, Bode, or Nyquist plots. The solution procedure is complex for multi-input, multi-output systems. Rosenbrock,[3] McFarlane,[4] and others have done much work in this area, though the practical application of these techniques is still quite difficult.

II. Properties of LQG and Classical Controllers

The LQG controllers have a fixed structure described previously. The closed-loop transfer function is of the form

Received Sept. 19, 1979; revision received Feb. 12, 1980. Copyright © American Institute of Aeronautics and Astronautics, Inc., 1980. All rights reserved.

Index categories: Guidance and Control; Spacecraft Dynamics and Control.

*Research Scientist and President.

(ω is the frequency)

$$x(j\omega) = (j\omega I - F - GC)^{-1} w(j\omega)$$
$$y(j\omega) = H(j\omega I - F - GC)^{-1} w(j\omega) \tag{12}$$

It has been shown by Anderson and Moore[5] and Athans and Safonov[6] that the controller has a 60 deg phase margin and 50% to infinite gain margin. The phase and gain margin propeties provide for a constant phase error in all channels and for individual variations in gain. The system may be extremely sensitive if two gains change in opposite directions. In addition, the phase and gain margin properties do not relate directly to parameter sensitivity. When a filter is used for state estimation, the gain and phase margin properties are no longer valid. In addition, the filter dynamics, dictated by specific noise characteristics, may be too fast, leading to interaction with unmodeled terms. Very definite attention must be given to the problem of filter design when estimated states are used in LQG controllers. The transfer functions of the closed-loop system when a filter is used for state estimation is given by

$$x(j\omega) = [j\omega I - F - GC(j\omega I - F - GC + KH)^{-1} KH]^{-1} w(j\omega)$$
$$y(j\omega) = Hx(j\omega) \tag{13}$$

Note that $F + GC - KH$ may have poles in the right half-plane, leading to right half-plane, closed-loop zeros which sometimes cause additional sensitivity.

The closed-loop transfer function has n poles and, at most $n-1$, zeros. Therefore, the frequency response may drop off as slowly as $1/\omega$ at high frequencies, where the model is not valid (higher-frequency modes are often neglected). This kind of response may be undesirable in many closed-loop systems. In addition, the controller has a tendency to push all responses to higher frequencies, resulting in more stringent actuator and sensor constraints. These LQG properties are a consequence of the optimization problem, which assumes the model is valid at all frequencies and for all deviations of the state variable.

The classical controllers, when properly designed, work well. The general form of the compensator matrix $C_c(s)$ provides enough flexibility for a variety of control design requirements. The major problem is the difficulty in obtaining the control law. The closed-loop transfer function between the output and the noise is

$$y(j\omega) = [I + T(j\omega) C_c(j\omega)]^{-1} T_w(j\omega) w(j\omega) \tag{14}$$

where $T_w(j\omega)$ is the noise to output transfer function.

LQG methods with frequency-shaped cost functionals are developed to incorporate good classical control properties in modern control design methods, such that automated computational procedures may be used to compute control laws which now require more difficult graphical approaches.

The next two sections present the theoretical background and a design algorithm for the frequency-shaping approach.

III. Frequency Shaping of Cost Functionals

To understand the concept of frequency shaping, it is necessary to write the standard LQG cost functional of Eq. (2) in the frequency domain. With infinite time horizon and no weighting on the final state, the cost functional may be written in the frequency domain using Parseval's theorem

$$J = \frac{1}{2} \int_{\infty}^{\infty} [x^*(j\omega) A x(j\omega) + u^*(j\omega) B u(j\omega)] \, d\omega \tag{15}$$

where * implies complex conjugate. Clearly, in this formulation the weighting matrices are not functions of frequency, i.e., the state and control excursions at all frequencies are considered equally unacceptable. In many systems, on the other hand, inputs in the neighborhood of a particular frequency are not desirable because of poor sensor, actuator, or model characteristics at that frequency. Historically, this constraint of constant weighting at all frequencies has resulted because of the difficulty of shaping the weighting functional with frequency in the conventional time domain LQG formulation. Representation of the cost functional in frequency domain provides a clue to the use of frequency shaping ideas in modern control theory techniques. Matrices A and B in Eq. (15) may be made functions of frequency to give a generalized cost functional

$$J = \frac{1}{2} \int_{\infty}^{\infty} [x^*(j\omega) A(j\omega) x(j\omega) + u^*(j\omega) B(j\omega) u(j\omega)] \, d\omega \tag{16}$$

where $A(j\omega)$ and $B(j\omega)$ are Hermitian matrices at all frequencies. It appears that a solution can be guaranteed if $B(j\omega)$ is positive definite and $A(j\omega)$ is positive semidefinite at all but a finite number of discrete frequencies (though this is not a necessary condition). It should be pointed out that even under these constraints the solution may not be easy to find and, in fact, may not even be causal. The total class of weighting functions for which a causal solution may be found will be subjects of future research.

Polynomial weighting matrices A and B are studied in the following section.

IV. Control Law Design

If the weighting functions $A(j\omega)$ and $B(j\omega)$ are assumed to be rational functions of squared frequency ω^2, a systematic control design procedure may be developed for positive semidefinite $A(j\omega)$ and positive definite $B(j\omega)$. This is not a serious limitation because a wide variety of functional forms may be approximated by ratios of polynomials. To develop a specific control design procedure, it is further assumed that $A(j\omega)$ has rank p and $B(j\omega)$ is positive definite with full rank q

$$A(j\omega) = P_1^*(j\omega) P_1(j\omega) \tag{17}$$
$$B(j\omega) = P_2^*(j\omega) P_2(j\omega) \tag{18}$$

where P_1 and P_2 are $p \times n$ and $q \times q$ rational matrices. Define

$$P_1(j\omega) x = x^1 \tag{19}$$
$$P_2(j\omega) u = u^1 \tag{20}$$

If $P_1(j\omega)$ is a ratio of polynomials in $j\omega$ and the number of zeros does not exceed the number of poles, Eq. (19) may be written as a system of differential equations with output x^1:

$$\dot{z}_1 = F_1 z_1 + G_1 x \qquad x^1 = H_1 z_1 + D_1 x \tag{21}$$

where D_1 is zero if the number of poles is at least one more than the number of zeros. Equation (20) may also be written in terms of a differential equation, again if the number of zeros does not exceed the number of poles.

$$\dot{z}_2 = F_2 z_2 + G_2 u \qquad \dot{u}^1 = H_2 z_2 + D_2 u \tag{22}$$

The dynamic Eq. (1) and the cost functional Eq. (16) may now be written in terms of an extended state vector.

$$\frac{d}{dt} \begin{bmatrix} x \\ z_1 \\ z_2 \end{bmatrix} = \begin{bmatrix} F & 0 & 0 \\ G_1 & F_1 & 0 \\ 0 & 0 & F_2 \end{bmatrix} \begin{bmatrix} x \\ z_1 \\ z_2 \end{bmatrix} + \begin{bmatrix} G \\ 0 \\ G_2 \end{bmatrix} u \tag{23}$$

$$J_{ss}=E(x^T z_1^T z_2^T u^T)$$

$$\times\begin{bmatrix} D_1^TD_1 & D_1^TH_1 & 0 & 0 \\ H_1^TD_1 & H_1^TH_1 & 0 & 0 \\ 0 & 0 & H_2^TH_2 & H_2^TD_2 \\ 0 & 0 & D_2^TH_2 & D_2^TD_2 \end{bmatrix}\begin{bmatrix} x \\ z_1 \\ z_2 \\ u \end{bmatrix} \tag{24}$$

Defining appropriate vectors and matrices, Eqs. (23) and (24) become

$$\dot{X}=F^1X+G^1u \tag{25}$$

$$J=\lim_{T\to\infty}\frac{1}{2T}\int_0^T [X^Tu^T]\begin{bmatrix} A^1 & N \\ N & B^1 \end{bmatrix}\begin{bmatrix} X \\ -- \\ u \end{bmatrix} dt \tag{26}$$

The control law is obtained by solving the following modified algebraic Riccati equation:

$$-SF^1-F^{1^T}S-A^1+(SG^1+N)[B^1]^{-1}(SG^1+N)^T=0 \tag{27}$$

and

$$u=[B^1]^{-1}(SG^1+N)^TX \tag{28}$$

Equation (28) is written in an equivalent form as

$$u=C_1x+C_2z_1+C_3z_2 \tag{29}$$

The generalized controller structure is then shown in Fig. 1. This controller has the form of a dynamic compensator. The transfer function between the control input u and the state x is

$$z_1(j\omega)=(j\omega I-F_1)^{-1}G_1x \tag{30}$$

$$z_2(j\omega)=(j\omega I-F_2)^{-1}G_2u \tag{31}$$

$$[I-C_3(j\omega I-F_2)^{-1}G_2]u(j\omega)$$

$$=[C_1+C_2(j\omega I-F_1)^{-1}G_1]^{-1}x(j\omega) \tag{32a}$$

or

$$u(j\omega)$$

$$=[I-C_3(j\omega I-F_2)^{-1}G_2][C_1+C_2(j\omega I-F_1)^{-1}G_1]x(j\omega) \tag{32b}$$

The compensator may be expressed in an equivalent form shown in Fig. 2. Note that the transfer functions between x^1 and u and u^1 and u are

$$x^1(j\omega)=[H_1(j\omega I-F_1)^{-1}G_1+D_1]u(j\omega) \tag{33}$$

$$u^1(j\omega)=[H_2(j\omega I-F_2)^{-1}G_2+D_2]u(j\omega) \tag{34}$$

Therefore, the poles of $P_1(j\omega)$ and $P_2(j\omega)$ show up as compensator poles and zeros, respectively, and directly influence the closed-loop transfer function. This provides a direct relationship between the form of the frequency-dependent shaping used in the cost function and the structure of the overall compensator.

If the number of zeros in $P_1(j\omega)$ exceeds the number of poles, Eq. (21) must be modified. For example, if $P_1(j\omega)$ has one more zero than poles, Eq. (21) may be written as

$$\dot{z}_1=F_1z_1+G_1x \qquad x^1=H_1z_1+D_1x+D_{11}\dot{x} \tag{35}$$

Using Eq. (1), this may be written as

$$\dot{z}_1=F_1z_1+G_1x$$

$$x^1=H_1z_1+D_1x+D_{11}(Fx+Gu)$$

$$=H_1z_1+(D_1+D_{11}F)x+D_{11}Gu \tag{36}$$

Therefore, when $P_1(j\omega)$ may have k_1 more zeros than poles, a more general form for Eq. (21) is

$$\dot{z}=F_1z_1+G_1x$$

$$x^1=H_1z_1+D_1x+\sum_{i=0}^{k_1-1}D_1^iu^{(i)} \tag{37}$$

where $u^{(i)}$ is the ith derivative of u. Equations (22-24) are also modified similarly.

V. Examples

Example 1: Control of Aircraft During Landing in Constant Lateral Winds

The equations of an aircraft are

$$\dot{x}=Fx+Gu+\Gamma w$$

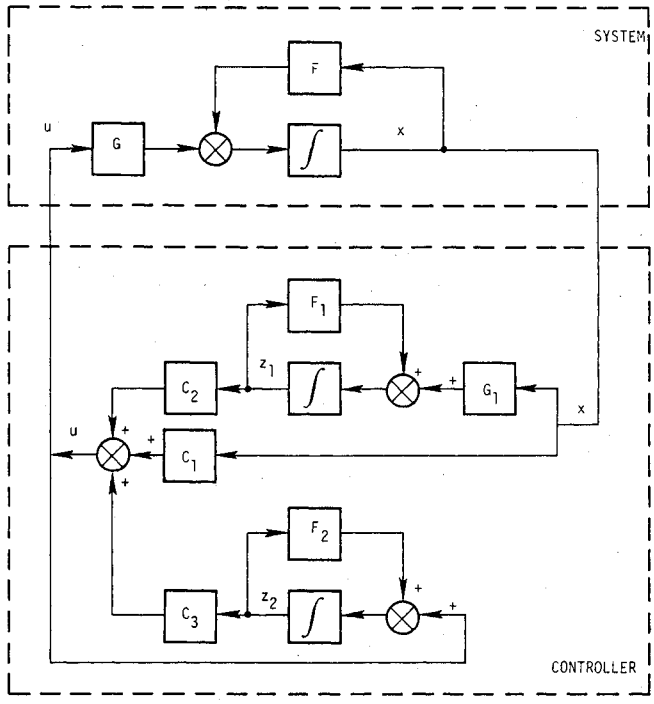

Fig. 1 Structure of the generalized controller.

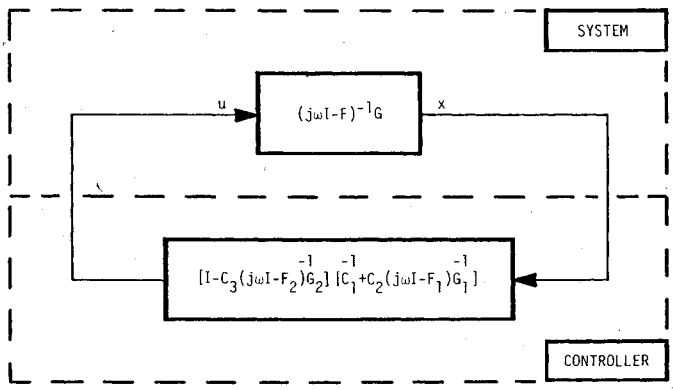

Fig. 2 Alternate representation of a frequency-shaped controller.

$x^T=[v,p,r,\phi]$, $u^T=[\delta a,\delta r]$, and w is constant lateral wind (v,p,r, and ϕ are lateral speed, roll rate, yaw rate, and roll angle; δa and δr are lateral inputs). Control laws based on standard LQG methods are of the form $u=Cx$ and, for any finite C, give a constant steady-state error. Constant biases correspond to errors at zero frequency. To reduce the steady-state error in v to zero, an additional term of the following forms should be added to the performance index v^2/ω^2. Defining $\xi=v/j\omega \rightarrow \dot{\xi}=v$, the additional term in the performance index is ξ^2. This is integral control!

There is a similar problem in many systems where the rates of change of control inputs affect system dynamics leading to control saturation. An example is the control of spacecraft attitude using control moment gyros. To avoid saturation, additional terms of the following form may be added to the performance index u^2/ω^2. This is input integral control to avoid saturation.

Example 2: Design of a Control System for an Overhead Crane (Fig. 3)

The equations of motion can be approximated for small θ

$$m\ddot{x}_1 = mg\sin\theta \approx mg(x_2-x_1)/l$$

$$m_1\ddot{x}_2 = f-mg\sin\theta \approx f-(m_1g/l)(x_2-x_1)$$

Consider a case in which $m=m_1=1000$ lb_m, $l=32$ ft, and $g=32$ ft-s^{-2}. The open-loop eigenvalues are at 0.0, 0.0, $\pm\sqrt{2}j$. The problem is to design a regulator to control the position of mass hanging from the crane without producing serious residual oscillations.

A standard cost functional is of the form

$$J=\lim_{T\to\infty}\frac{1}{T}\int_0^T (a_1x_1^2+a_2x_2^2+u^2)\,dt$$

A good response is obtained for $a_1=1$ and $a_2=0$. The time histories of x_1, x_2, and u are shown in Fig. 4. Notice that the hanging mass continues to oscillate at about $\sqrt{2}$ rad-s^{-1}. Improved response can be obtained by placing some penalty on velocities.

The most improvement was obtained by using frequency shaping methods. Since there is significant oscillation around $\sqrt{2}$ rad-s^{-1}, it is useful to include a term of the form $l^2\theta^2/(\omega^2-2)^2$ in the performance index. This term is included with a unity weighting. The resulting controller transfer function is

$$u(s)=\left[-0.64s+1.1+\frac{0.85+0.38s}{s^2+2}\right]x_1(s)$$

$$+\left[-2.2s-2.1+\frac{0.85+0.38s}{s^2+2}\right]x_2(s)$$

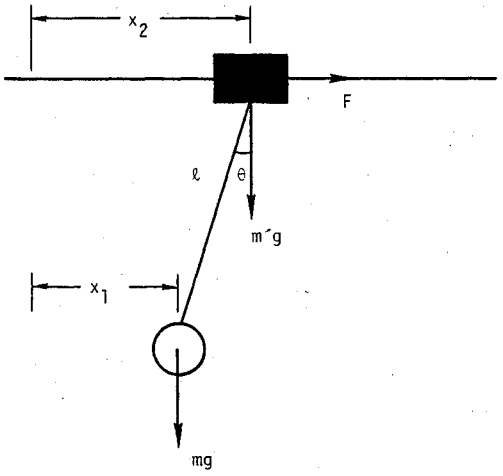

Fig. 3 Dynamics of an overhead crane.

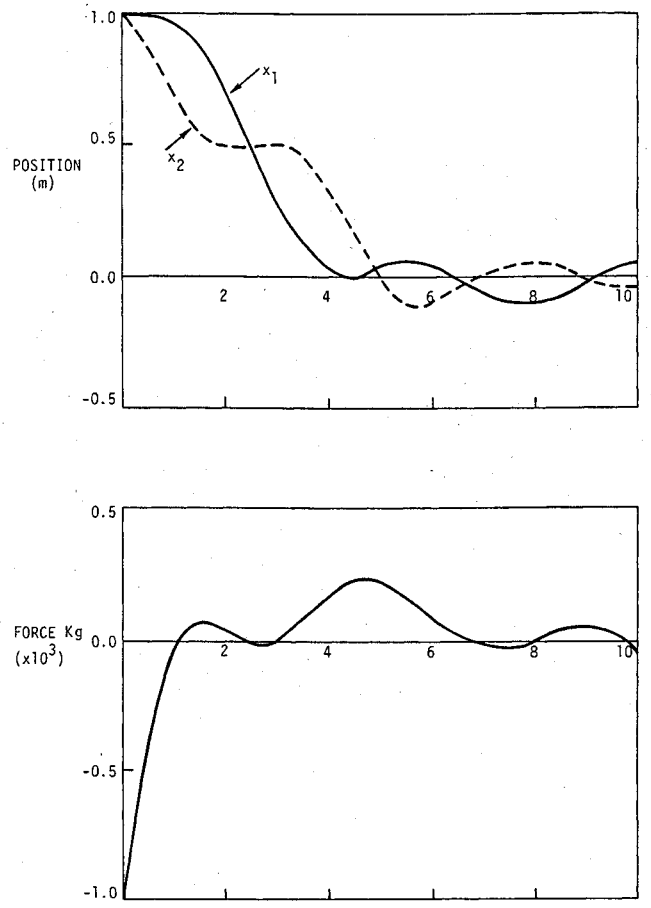

Fig. 4 Time histories of responses with cost functional $(x_1^2+u^2)$.

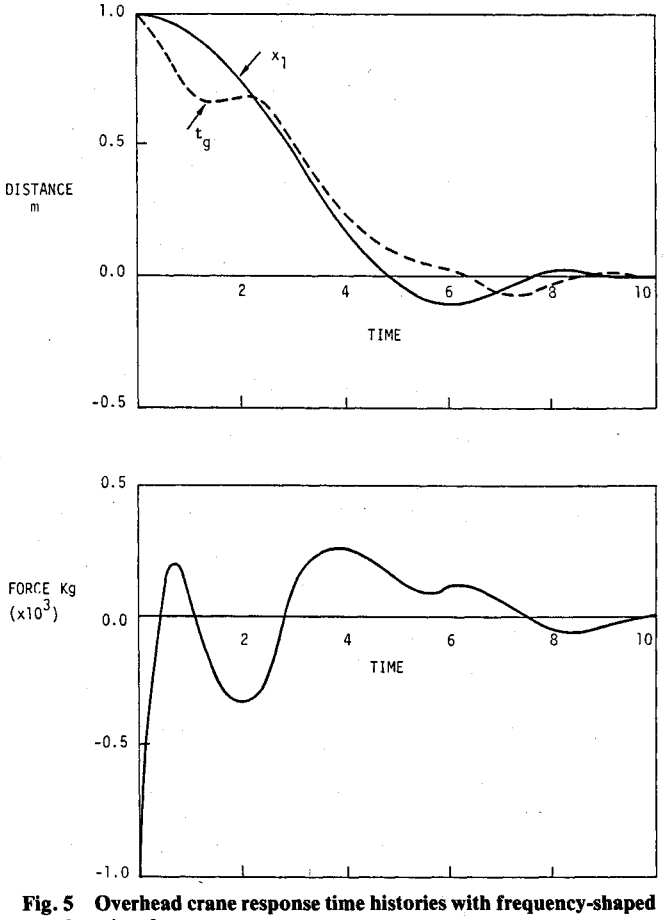

Fig. 5 Overhead crane response time histories with frequency-shaped cost functional.

Time history of responses starting from an initial condition error of 1 m are shown in Fig. 5. Notice that the maximum control input is the same. Major differences in the applied control input occur throughout the trajectory. At the end of 10 s, the amplitude of oscillation is an order of magnitude smaller than it is in Fig. 4. This shows the effectiveness of frequency shaping methods.

Example 3: Vibration Control of a Helicopter

Helicopters suffer from significant vibration at $N\Omega$, $2N\Omega$,..., etc., discrete frequencies where N is the number of blades in the rotor and Ω is the rotational frequency. In the example considered here, the equations of motion describing the behavior of a helicopter near the vibration frequency are assumed to be

$$\begin{bmatrix} \dot{w} \\ \dot{\beta}_0 \\ \ddot{\beta}_0 \end{bmatrix} = \begin{bmatrix} -0.0839 & -241.4 & -11.23 \\ 0 & 0 & 1 \\ 0.1186 & -142.7 & -1.137 \end{bmatrix} \begin{bmatrix} w \\ \beta_0 \\ \dot{\beta}_0 \end{bmatrix} + \begin{bmatrix} -2.82 \\ 0 \\ 2.2 \end{bmatrix} \delta_{\text{coll}} + \begin{bmatrix} 0.1 \\ 0 \\ -0.2 \end{bmatrix} \delta_{\text{vib}}$$

where w is the vertical speed (ft/s), β_0 is the coning angle of the blades (rad), δ_{coll} is the collective pitch control (in.), and δ_{vib} is the oscillating disturbance (force).

Consider vibration at 20 rad-s^{-1}:

$$\delta_{\text{vib}} = 0.2 \cos(20\, t)$$

where t is time in seconds.

The way to avoid vibration is to minimize response at $\omega_v = 20$ rad-s^{-1}. A frequency-shaped cost functional of the following form may be selected:

$$J = \frac{1}{2\pi} \int_{-\infty}^{\infty} Q_z |P(j\omega)|^2 |w(j\omega)|^2 + R |\delta_{\text{coll}}(j\omega)|^2 d\omega$$

where

$$P(j\omega) = \frac{j\,400\omega}{400 - \omega^2 + j\,40\,\xi\omega}$$

and ξ is a design parameter. The cost functional is converted into a time-domain formulation by adding the following states:

$$\frac{d}{dt}\begin{bmatrix} Z_1 \\ Z_2 \end{bmatrix} = \begin{bmatrix} 0 & 1 \\ -400 & -40\xi \end{bmatrix} \begin{bmatrix} z_1 \\ z_2 \end{bmatrix} + \begin{bmatrix} 0 \\ 400 \end{bmatrix} w$$

This equation, combined with the helicopter model, specifies the plant description to be used with the performance index described in Eq. (4). The augmented state description is

$$\left[\begin{array}{c} \dot{w} \\ \dot{\beta}_0 \\ \ddot{\beta}_0 \\ \hline \dot{z}_1 \\ \dot{z}_2 \end{array}\right] = \left[\begin{array}{ccc:cc} -0.0839 & -241.4 & -11.23 & 0 & 0 \\ 0 & 0 & 1 & 0 & 0 \\ 0.1186 & -142.7 & -1.137 & 0 & 0 \\ \hdashline 0 & 0 & 0 & 0 & 1 \\ 400 & 0 & 0 & -400 & -40\,\xi \end{array}\right] \left[\begin{array}{c} w \\ \beta_0 \\ \dot{\beta}_0 \\ \hline z_1 \\ z_2 \end{array}\right] + \left[\begin{array}{c} -2.82 \\ 0 \\ 2.2 \\ \hline 0 \\ 0 \end{array}\right] \delta_{\text{coll}}$$

The optimal control law is of the form

$$\delta_{\text{coll}} = C_w w + C_\beta \beta_0 + C_{\dot{\beta}} \dot{\beta} + C z_1 + C_2 z_2$$

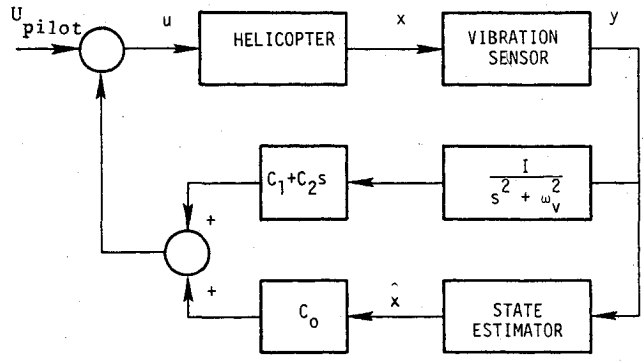

Fig. 6 Structure of helicopter vibration controller.

An implementation of this vibration controller is shown in Fig. 6. The vibration level at a point in the helicopter after the controller is switched on is shown in Fig. 7 ($\xi = 0.01$). Even though ξ can be set to zero, a small value of ξ was used to minimize sensitivity to parameter variations.†

Example 4: Control of Structures

Dynamics of structures is described by a set of partial differential equations. Finite-order model representations are valid only at low frequencies. We show how frequency shaping methods are used to design control laws for models valid only at low frequencies.

Consider a freestanding pyramid where we wish to control line-of-sight errors at the apex (Fig. 8). The size of various elements are given in Tables 1 and 2.‡ We have an eight-mode model representing the behavior of the system below 1 Hz. These actuators and three sensors are available to actively increase damping ratios of specific modes which affect open line-of-sight errors. All modes have an open-loop damping ratio of 0.5%.

Since the model is vsalid only at low frequencies, it is desirable to minimize control and state activities above 1 Hz. This may be achieved by a control weighting matrix which increases with frequency, for example,

$$B(j) = A_B(\omega^2 + \omega_0^2)$$

Λ_β is a diagonal matrix with elements b_1, b_2, and b_3. By selecting ω_0 at 0.5 Hz, the control weighting at 1.5 Hz is five times higher than at 0.5 Hz. The control weighting is written equivalently as

$$(u^T \Lambda_B u)(\omega^2 + \omega_0^2) = v^T \Lambda_B v$$

where $\dot{u} + \omega_0 u = v$. The line-of-sight control requires increased damping in modes 1, 2, 4, and 5. This is achieved by state weighting of the form

$$0.5(q_1^2 + q_2^2 + q_4^2 + \dot{q}_1^2 + \dot{q}_2^2 + \dot{q}_4^2) + (q_3^2 + \dot{q}_3^2)$$

†Recent research has shown that $\xi = 0$ can be used without increase in sensitivity.

‡This example was developed by R. Strunce and his associates at Charles Stark Draper Laboratory, Cambridge, Mass.

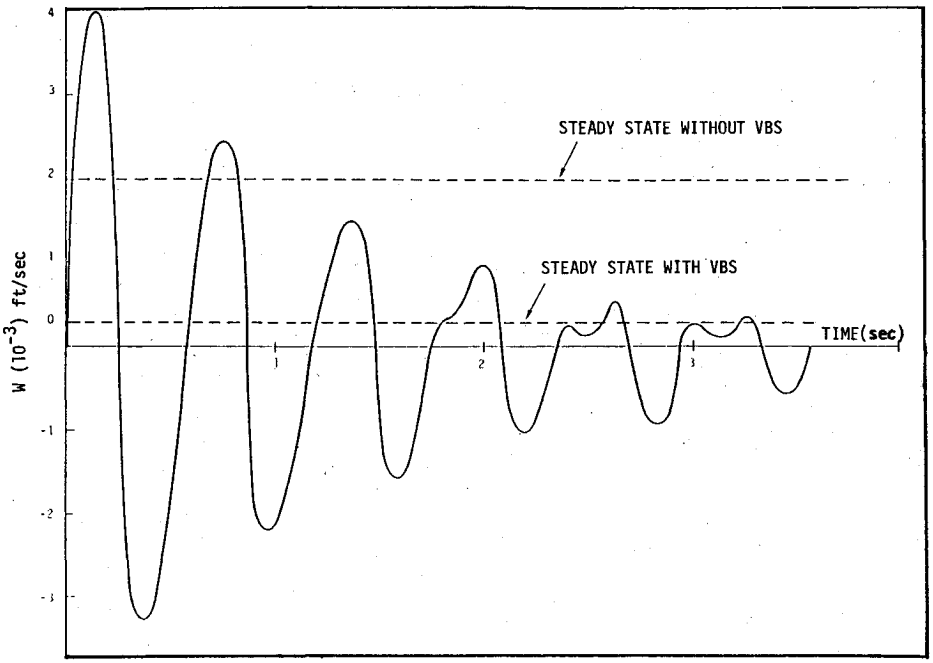

Fig. 7 Lateral vibration vs time with the vibration suppression regulator.

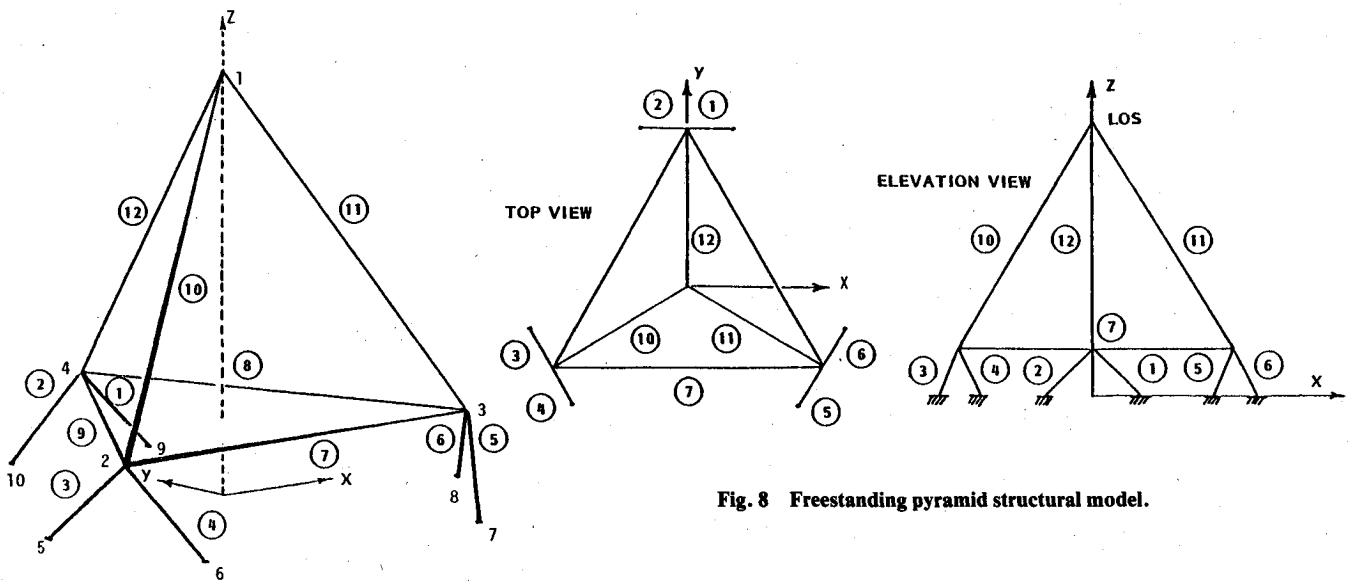

Fig. 8 Freestanding pyramid structural model.

Table 1 Cross-sectional areas

Truss element no.	Area
1	100
2	100
3	100
4	100
5	100
6	100
7	1000
8	1000
9	1000
10	1000
11	100
12	100

Table 2 Structural node coordinates

Node	X	Y	Z
1	0.0	0.0	10.165
2	−5.0	−2.887	2.0
3	5.0	−2.887	2.0
4	0.0	5.7735	2.0
5	−6.0	−1.1547	0.0
6	−4.0	−4.6188	0.0
7	4.0	−4.6188	0.0
8	6.0	−1.1547	0.0
9	2.0	5.7735	0.0
10	−2.0	5.7735	0.0

q_i is the modal deflection corresponding to the ith mode and b_1, b_2, and b_3 are all set at 0.01.

Table 3 shows the closed-loop eigenvalues for the eight-mode design model and the twelve-mode evaluation model. Because of the low control activity at high frequencies, the damping ratios of unmodeled high-frequency modes have small perturbations.

When a comparable design was carried out without frequency shaping of state and control weighting matrices, the perturbations in the unmodeled eigenvalues were so large that some of the modes were unstable.

Discussion

We have shown some simple applications of frequency shaping methods. The method is much more powerful and is being applied to many complex problems.

Table 3 Damping ratios for design and evaluation models

	8-Mode model		12-Mode model	
Frequency, Hz	Controller	Filter	Controller	Filter
0.214	.109	.173	.110	.173
0.265	.125	.216	.124	.217
0.460	.033	.101	.0332	.098
0.471	.126	.167	.139	.155
0.541	.125	.158	.118	.163
0.669	.00604	.045	.0060	.045
0.742	.00550	.046	.0055	.046
0.757	.0192	.005	.0193	.005
1.36	...	...	.0059	...
1.47	...	...	.0044	...
1.64	...	...	.0044	...
2.05	...	...	.0049	...

A reviewer provides an interesting interpretation of the controllers of examples 2, 3, and 4. Examples 2 and 3 give a "virtual tuned vibration absorber," while example 4 gives a "virtual actuator dynamics."

VI. Conclusions

Frequency shaping of quadratic cost functionals can provide additional flexibility in developing control laws using modern control theory techniques. For good design, the particular selection of weighting functions depends on 1) model validity, 2) actuator/sensor characteristics, 3) control objectives, and 4) disturbance spectrum. Examples are presented to demonstrate the effectiveness of the proposed approach.

The design procedure for frequency-shaped weighting on state and control law is implemented by linear elements with memory.

The frequency-shaping concept has been extended for state estimation with models valid within a finite frequency range and with finite bandwidth sensors. These ideas may also be used in parameter identification.

Acknowledgments

This research was supported by the Office of Naval Research under Contract N00014-77-C-0247. Results reported in the paper were generated by J. Fuller, S. Bangert, and S. DuHamel.

References

[1] Bryson, A.E. and Ho, Y.C., *Applied Optimal Control,* Xerox, Blaisdell, Mass., 1974.

[2] Doyle, J.C., "Guaranteed Margins for LQG Regulators," *IEEE Transactions on Automatic Control,* Vol. AC-23, No. 4, Aug. 1978, pp. 756-757.

[3] Rosenbrock, H.H., *Computer Aided Control System Design,* Academic Press, New York, 1974.

[4] McFarlane, A.G.J. and Postlethwaite, I., "The Generalized Nyquist Stability Criteria and Multivariable Root Loci," *International Journal of Control,* No. 25, 1977, pp. 81-127.

[5] Anderson, B.D.O. and Moore, J.B., *Linear Optimal Control,* Prentice Hall, Englewood Cliffs, N.J., 1971.

[6] Safonov, M.G. and Athans, M., "Gain and Phase Margin for Multiloop LQG Regulators," *IEEE Transactions on Automatic Control,* Vol. AC-22, April 1977, pp. 173-179.